

# In Situ-Formed Fibrin Hydrogel Scaffold Loaded With Human Umbilical Cord Mesenchymal Stem Cells Promotes Skin Wound Healing

Cell Transplantation  
Volume 32: 1–12  
© The Author(s) 2023  
Article reuse guidelines:  
sagepub.com/journals-permissions  
DOI: 10.1177/09636897231156215  
journals.sagepub.com/home/cll  


Lvzhong Hu<sup>1\*</sup>, Jinhua Zhou<sup>1\*</sup>, Zhisong He<sup>2\*</sup>, Lin Zhang<sup>1</sup>, Fangzhou Du<sup>3</sup>, Mengting Nie<sup>3,4</sup>, Yao Zhou<sup>1</sup>, Hang Hao<sup>3</sup>, Lixing Zhang<sup>3</sup>, Shuang Yu<sup>3,5,6</sup>, Jingzhong Zhang<sup>3,5,6</sup>, and Youguo Chen<sup>1</sup>

## Abstract

Healing of full-thickness skin wounds remains a major challenge. Recently, human umbilical cord mesenchymal stem cells (hUC-MSCs) were shown to possess an extraordinary potential to promote skin repair in clinical settings. However, their low survival rate after transplantation limits their therapeutic efficiency in treating full-thickness skin wounds. Hydrogels are considered an ideal cell transplantation vector owing to their three-dimensional mesh structure, good biosafety, and biodegradation. The objective of this study was to investigate the skin wound healing effect of a fibrin hydrogel scaffold loaded with hUC-MSCs. We found that the fibrin hydrogel had a three-dimensional mesh structure and low cytotoxicity and could prolong the time of cell survival in the peri-wound area. The number of green fluorescent protein (GFP)-labeled hUC-MSCs was higher in the full-thickness skin wound of mice treated with hydrogel-hUC-MSCs than those of mice treated with cell monotherapy. In addition, the combination therapy between the hydrogel and hUC-MSCs speed up wound closure, its wound healing rate was significantly higher than those of phosphate-buffered saline (PBS) therapy, hydrogel monotherapy, and hUC-MSCs monotherapy. Furthermore, the results showed that the combination therapy between hydrogel and hUC-MSCs increased keratin 10 and keratin 14 immunofluorescence staining, and upregulated the relative gene expressions of epidermal growth factor (EGF), transforming growth factor- $\beta$ 1 (TGF- $\beta$ 1), and vascular endothelial growth factor A (VEGFA), promoting epithelial regeneration and angiogenesis. In conclusion, the fibrin hydrogel scaffold provides a relatively stable sterile environment for cell adhesion, proliferation, and migration, and prolongs cell survival at the wound site. The hydrogel-hUC-MSCs combination therapy promotes wound closure, re-epithelialization, and neovascularization. It exhibits a remarkable therapeutic effect, being more effective than the monotherapy with hUC-MSCs or hydrogel.

## Keywords

human umbilical cord mesenchymal stem cells, hydrogel, fibrin, skin wound healing

<sup>1</sup> Department of Obstetrics and Gynecology, The First Affiliated Hospital of Soochow University, Suzhou, China

<sup>2</sup> Department of Cardiovascular Medicine, The First Affiliated Hospital of Soochow University, Suzhou, China

<sup>3</sup> Suzhou Institute of Biomedical Engineering and Technology, Chinese Academy of Sciences, Suzhou, China

<sup>4</sup> School of Life Science and Technology, Changchun University of Science and Technology, Changchun, China

<sup>5</sup> Zhengzhou Institute of Engineering and Technology Affiliated to SIBET, Zhengzhou, China

<sup>6</sup> Xuzhou Medical University, Xuzhou, China

\*These authors contributed equally to this work.

Submitted: April 5, 2022. Revised: January 15, 2023. Accepted: January 18, 2023.

## Corresponding Authors:

Shuang Yu, Suzhou Institute of Biomedical Engineering and Technology, Chinese Academy of Sciences, Suzhou 215163, China.  
Email: yush@sibet.ac.cn

Jingzhong Zhang, Suzhou Institute of Biomedical Engineering and Technology, Chinese Academy of Sciences, Suzhou 215163, China.  
Email: zhangjz@sibet.ac.cn

Youguo Chen, Department of Obstetrics and Gynecology, The First Affiliated Hospital of Soochow University, Suzhou 215006, China.  
Email: chenyouguo@suda.edu.cn



## Introduction

The skin is the largest organ of the human body and the first barrier against the external environment, preventing external damage and microbial invasion and maintaining the normal physiological environment<sup>1-3</sup>. Once the skin is damaged, the wound disables the barrier function and in severe cases, even threatens people's lives. Full-thickness skin wound can result from all kinds of injuries, such as acute trauma, chronic ulcers, and deep burns, and cause many physiological and functional problems<sup>4</sup>.

In recent years, the advantages of mesenchymal stem cell (MSC) transplantation for skin wound healing have attracted extensive attention in skin-related research. Researchers have proved that MSCs play important roles in all stages of wound healing<sup>5-9</sup>. However, for overcoming inconvenience, such as invasive collection, short survival time, and immunological rejection, further research is needed.

MSCs can be obtained from various sources, including the bone marrow, adipose tissue, umbilical cord, Wharton's jelly, and placenta<sup>10</sup>. Among them, human umbilical cord mesenchymal stem cells (hUC-MSCs) have the advantages of painless collection, no associated ethical dispute, fast self-renewal, low immunogenicity, and more prospects of clinical applications than other types of MSCs<sup>11-13</sup>. hUC-MSCs can accelerate wound healing, inhibit the inflammatory response, promote re-epithelialization, and increase angiogenesis without serious complications or adverse reactions<sup>14-19</sup>.

At present, traditional cotton medical gauze is widely used as clinical routine dressing. However, it has some inevitable disadvantages, such as limited use, poor absorption properties, and the need for frequent replacement, which may cause secondary trauma. Biological dressings, such as pig skin, carry the risk of spreading bacteria and viruses and immunological rejection<sup>20-23</sup>. Alternatively, hydrogels are considered a better material for wound treatment. Hydrogels have good biocompatibility, can prevent the loss of water and body fluid from wounds, and owing to their biodegradability, secondary damage during dressing change can be avoided. They are easy to use, especially suitable for irregular wounds, and can resist bacterial invasion<sup>24-26</sup>. Moreover, their three-dimensional mesh structure and low cytotoxicity provide a suitable environment for cell adhesion and proliferation and prolong the survival of cells around the wound. Thus, hydrogels have prospects of broad application in the fields of tissue engineering and drug-controlled release<sup>27-30</sup>.

With its excellent biocompatibility and safety, fibrin hydrogel is authorized for human use by the Food and Drug Administration<sup>31-33</sup>. In this study, we engineered a fibrin hydrogel scaffold, formed by the interaction of fibrinogen and thrombin. This scaffold was loaded with hUC-MSCs with the purpose of being implanted into the wound area for the treatment of full-thickness skin defects. Using a mouse model, we explored the wound healing effects of this new fibrin hydrogel scaffold loaded with hUC-MSCs.

## Materials and Methods

### Synthesis of the Fibrin Hydrogel Scaffold

Freeze-dried fibrinogen powder (F8051, Solarbio, China) was dissolved in sterilized water to prepare a fibrinogen solution 10 mg/ml. Freeze-dried thrombin powder (T8021, Solarbio, China) was dissolved in calcium ion solution (containing 300 mmol/l sodium chloride, 40 mmol/l calcium chloride) to prepare a thrombin solution 25 U/ml. Fibrinogen and thrombin solutions were mixed at a ratio of 1:1 (v/v) to synthesize fibrin hydrogel scaffolds.

### Characterization of the Fibrin Hydrogel Scaffold

*Characterization by field emission scanning electron microscopy.* Fibrin hydrogel scaffolds were characterized using field emission scanning electron microscopy (FESEM; S4800, Hitachi, Japan). The fibrin hydrogel was transformed into a lyophilized scaffold using a vacuum freeze dryer (LICHEN LC-10N-50C), fixed on a copper bar, and sprayed with gold. Then, the morphology of the hydrogel scaffold was observed via FESEM.

*In vitro degradation of the fibrin hydrogel scaffold.* Fibrin hydrogel scaffolds were immersed in phosphate-buffered saline (PBS) and placed in a biosafety cabinet. Scaffolds were periodically taken out to drain off surface moisture, and the remaining mass was weighed. On days 0, 3, 7, 10, and 14 after scaffold formation, the degradation rate was calculated using the following formula:

$$\text{Degradation rate (\%)} = (W_i - W_r) / W_i \times 100\%,$$

where  $W_i$  is the initial weight of the hydrogel and  $W_r$  is the remaining weight of the hydrogel.

### Fibrin Hydrogel Scaffold Toxicity Analysis

The cytotoxicity of the fibrin hydrogel was determined using cell counting kit-8 (CCK-8) assay. Hydrogels were pre-treated with culture media in an incubator at 37°C and 5% CO<sub>2</sub> for 24 h. The supernatant was collected and filter-sterilized resulting in the 100% hydrogel extract. Furthermore, the extract was used to culture hUC-MSCs for 24 or 48 h. Subsequently, 10 µl CCK-8 solution (Dojindo, Japan) was added to each well of a 96-well culture plate, and the plate was incubated for 4 h in the incubator. The absorbance was measured immediately at 450 nm, using a microplate reader.

### Isolation and Culture of hUC-MSCs

Human umbilical cord tissues were obtained from cesarean sections performed at the Obstetrics and Gynecology Department of the First Affiliated Hospital of Soochow

University (Suzhou, China). Informed consent was obtained from all patients. The human umbilical cord tissue sampling schemes were approved by the Ethics Review Committee of the First Affiliated Hospital of Soochow University. Briefly, several segments of the fresh umbilical cord tissue (3 cm each) were collected under aseptic conditions in the operating room, rinsed several times with sterile saline to remove blood clots, placed in sterile boxes containing PBS supplemented with 100 U/ml penicillin and 100 µg/ml streptomycin on ice, and transported to the laboratory immediately. The umbilical cords were washed again several times with PBS supplemented with 100 U/ml penicillin and 100 µg/ml streptomycin and cut into 1 mm<sup>3</sup> fragments with a surgical scissor. The fragments were placed in a Petri dish and a small amount of Dulbecco's Modified Eagle Medium and Ham's Nutrient Mixture F-12 (DMEM/F12) (C11330500BT, Gibco, USA) with 10% fetal bovine serum (FBS) (10099-141, Gibco, USA) was added. The dish was incubated in an incubator at 37°C and 5% CO<sub>2</sub>, and medium was added every 3 days. The fragments were removed when many cells migrated out. The cells were passaged when they reached 80% confluence. Before transplantation, hUC-MSCs were infected with lentivirus carrying the enhanced GFP reporter gene. hUC-MSCs at passages 2–5 were used for the following experiments.

### Flow Cytometry

hUC-MSCs surface antigens were detected between the second and fifth passages, using flow cytometry. In total, 1 × 10<sup>6</sup> suspended cells were incubated with 0.5% bovine serum albumin (BSA)/PBS at 4°C for 30 min to block non-specific antigens. The cells were lucifugally incubated with fluorescein isothiocyanate (FITC)-labeled anti-mouse CD45 (Biolegend) and CD90 (Biolegend), as well as phycoerythrin (PE)-labeled anti-mouse CD34 (Biolegend) and CD105 (Biolegend), at 4°C for 60 min. The cells were washed twice with 0.5% BSA/PBS and resuspended in 200 µl of 0.5% BSA/PBS and analyzed using a flow cytometer (BD, LSRFortessa).

### Adipogenic and Osteoblastic Differentiation of hUC-MSCs

Adipogenic and osteoblastic differentiation assays were performed to detect the multidirectional differentiation potential of the hUC-MSCs. Adipogenic differentiation was induced using adipogenic induction medium (Stemcell, Canada). The medium was changed every 3 days and oil red O staining was performed on day 14. Osteogenic differentiation was induced using osteogenic induction medium (Cyagen, USA). The medium was changed every 3 days, and alizarin red staining was performed on day 21.

### Wound Model

All animal procedures were conducted following the provisions of the National Institutes of Health Guide for the Care and Use of Laboratory Animals. The protocol was approved by the Ethics Review Committee of the First Affiliated Hospital of Soochow University. Briefly, 72 female-specific pathogen-free class BALB/c mice aged 8 weeks were randomly divided into four groups: PBS therapy ( $n = 18$ ); hydrogel monotherapy group ( $n = 18$ ); hUC-MSCs monotherapy group ( $n = 18$ ); and hydrogel-hUC-MSCs combination group ( $n = 18$ ). Using an anesthesia machine (RWD, R540, China), mice were anesthetized with isoflurane at an initial high concentration (2% isoflurane, 2 l/min), which was further lowered (0.5%–1% isoflurane, 1 l/min). Mice were placed on a heating pad to keep them warm during the surgery. After removal of the dorsal hair with a shaver and depilatory cream, entoiodine was applied three times to disinfect the back skin. After disinfection, the back skin was covered with antibacterial film (Drape Antimicrob 35 × 35 cm BX10 6640EZ, 3M, USA) to avoid skin retraction. Next, full-thickness skin wounds with a diameter of 8 mm were established at the midline of the back of each mouse using a skin perforator. Then, PBS, fibrin hydrogel, hUC-MSCs (resuspended with PBS) or fibrin hydrogel loaded with hUC-MSCs were injected into the center of the wound and its periphery, respectively. In the hydrogel monotherapy group, fibrinogen and thrombin solutions were injected into the wound successively to synthesize the fibrin hydrogel scaffold *in situ*. In the hydrogel-hUC-MSC combination group, hUC-MSCs were resuspended with fibrinogen solution, then the resuspended suspension and thrombin solution were injected into the wound successively to synthesize *in situ* the fibrin hydrogel loaded with hUC-MSCs. The total injection volume for each animal was 20 µl, and the cell number was 3 × 10<sup>5</sup> per injection. After injection, all wounds were covered with another antibacterial film to avoid the dislocation of scaffolds or infection<sup>34</sup>. There were six mice for each time point in each group, and a total of 12 wounds for each time point. According to our unpublished data, the cells' ability to repair wounds lasts for about 7 days, so that, a second dose was administered on day 7. Mice were kept in separate cages with free access to food and water and observed daily throughout the experiment. On days 0, 3, 7, 10, and 14 after the surgery, wounds were photographed with a digital camera, and the healing was evaluated by calculating the area of the wound using ImageJ 1.47v software. The wound healing rate was calculated using the following formula:

$$\text{wound healing rate (\%)} = (A_o - A_u) / A_o \times 100\%,$$

where  $A_o$  is the original wound area and  $A_u$  is the unhealed wound area.

## Histological Analysis

On days 3, 7, and 14 after the surgery, the wound and surrounding tissues (diameter = 1 cm) were excised and fixed in 4% paraformaldehyde for 24 h. Samples were dehydrated in a graded ethanol series (70–100%) and cut into 6  $\mu\text{m}$ -thick serial

paraffin sections. According to the standard procedures, samples were stained with either hematoxylin and eosin (H&E) or immunofluorescent staining, including GFP (Abcam), keratin 10 (K10) (Abcam), and keratin 14 (K14) (Abcam). Then, the ratio of wound re-epithelialization length was calculated according to H&E staining results using the following formula:

$$\text{Re-epithelialization length ratio (\%)} = \frac{\text{length of epidermis extending inward}}{\text{length between the wound edges on both sides}} \times 100\%.$$

## Reverse Transcription Polymerase Chain Reaction

Total RNA was extracted from the lesioned tissue using TRIzol reagent (Invitrogen, America) according to the manufacturer's protocol. Next, the total extracted RNA was used to synthesize cDNA using the PrimeScript RT Master Mix (TaKaRa, RR036A, Japan). Reverse transcription polymerase chain reaction (RT-PCR), using TB Green Premix Ex Taq (TaKaRa, RR420A, Japan), cDNA, nuclease-free water, and the primers described below, was performed using an Applied Biosystems QuantStudio 7 Flex Real-time PCR system (Applied Biosystems, USA) with the following temperature profile: 95°C for 10 min, 40 cycles at 95°C for 15 s, and 60°C for 30 s. Primer sequences were as follows: mouse vascular endothelial growth factor A (VEGFA) forward 5'-GAACCAGACCTCTCACCGGAA-3', reverse 5'-GACCCAAAGTGCTCCTCGAAG-3' (GENEWIZ); mouse epidermal growth factor (EGF) forward 5'-CATCATGGTGGTGGCTGTCTG-3', reverse 5'-CACTTCCGCTTGCTCATCA-3' (GENEWIZ); mouse transforming growth factor- $\beta$ 1 (TGF- $\beta$ 1) forward 5'-CCCTATATTTGAGCCTGGA-3', reverse 5'-CTTGCGACCCACGTAGTAGA-3' (GENEWIZ); and mouse GAPDH forward 5'-AGGTCGGTGTGAACGGATTTG-3', reverse 5'-TGTAGCCATGTAGTTGAGGTCA-3' (GENEWIZ).

## Statistical Analysis

Statistical analysis was performed using GraphPad Prism 7.0 software. All data were presented as mean  $\pm$  standard error of the mean. Differences among the groups were assessed using one-way analysis of variance (ANOVA) followed by post hoc tests. A value of  $P < 0.05$  was considered statistically significant (significance levels: \* $P < 0.05$ , \*\* $P < 0.01$ , and \*\*\* $P < 0.001$ ).

## Results

### Synthesis and Characterization of the Fibrin Hydrogel Scaffold

Fibrin hydrogel scaffolds are formed through combining fibrinogen and thrombin solutions at a ratio of 1:1 (v/v)<sup>33</sup>.

Thrombin cuts fibrinopeptide A of the  $\alpha$  chain N-terminal region and fibrinopeptide B of  $\beta$  chain N-terminal region on the E domain of fibrinogen to produce fibrin monomers. Fibrin monomers are then bound via non-covalent bonds to form soluble fibrin polymers. With the participation of calcium ions, the adjacent fibrins undergo rapid covalent cross-linking, forming an insoluble and stable fibrin hydrogel. The whole process completes within a few seconds (Fig. 1A)<sup>31–33</sup>. This process simulates hemostasis in the body. The morphology of the fibrin hydrogel scaffold with a porous three-dimensional mesh microstructure was demonstrated using FESEM (Fig. 1B). CCK-8 assay showed the viability of hUC-MSCs seeded in fibrin hydrogels (Fig. 1C). Compared with DMEM/F12 medium-containing control, the extraction medium of fibrin hydrogels did not show any obvious toxicity. The crosslinked fibrin degraded slowly into fibrin degradation products (Fig. 1D). The integrity of the fibrin hydrogel was maintained for at least 1 week, after which the hydrogel degraded gradually within 2 weeks (Fig. 1E, F). These results showed that the fibrin hydrogel scaffold had a relatively high level of biological safety, good biodegradability, and a porous three-dimensional mesh structure, which provided a suitable environment for cell adhesion and proliferation.

### hUC-MSCs Possess the Characteristics of Stem Cells and Multidirectional Differentiation Potential

hUC-MSCs were evaluated in terms of plastic adherence, specific surface antigen expression, and multidirectional differentiation potential<sup>35</sup>. When maintained in standard culture conditions, hUC-MSCs were spindle-shaped and plastic-adherent (Fig. 2A). Oil red O (Fig. 2B) and alizarin red (Fig. 2C) stainings showed the formation of lipid droplets and mineralized nodules, respectively, which confirmed adipogenic and osteogenic differentiation abilities of hUC-MSCs. Moreover, flow cytometry demonstrated that these cells were positive for CD90 (> 99%) (Fig. 2D) and CD105 (> 97%) (Fig. 2E), whereas negative for CD34 (> 99%) (Fig. 2F) and CD45 (> 99%) (Fig. 2G). Thus, hUC-MSCs possessed the basic characteristics of MSCs, including the potential of multidirectional differentiation.

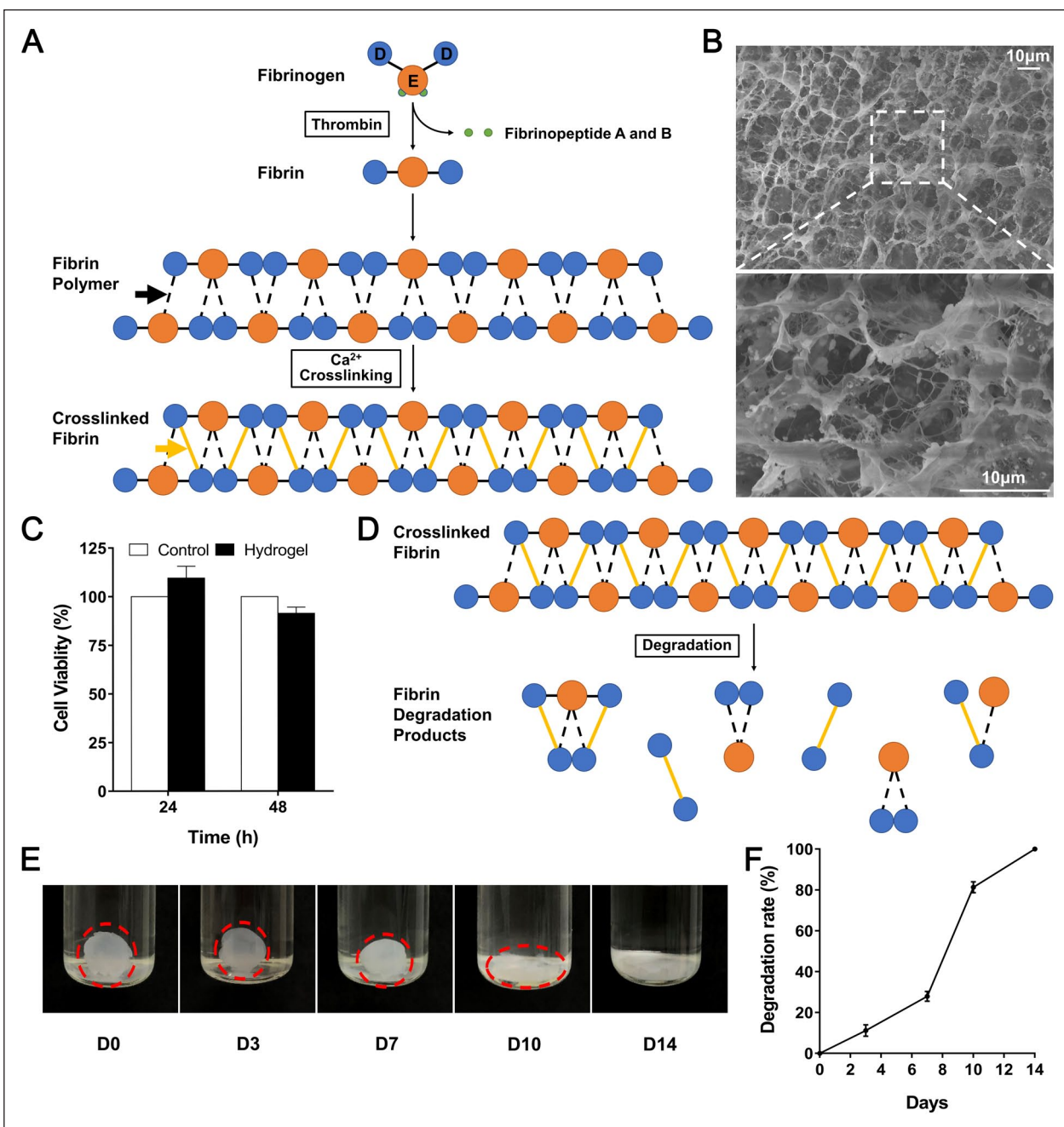


**Figure 1.** Synthesis and characterization of fibrin hydrogel scaffold. (A) Schematic diagram of fibrinogen and thrombin combining to form the fibrin hydrogel. (B) Representative field emission scanning electron microscopy image of fibrin hydrogel. (C) Cytotoxicity of hydrogel on human umbilical cord mesenchymal stem cells incubated in DMEM/F12 at 24 and 48 h (D) Schematic diagram of hydrogel degradation. (E) *In vitro* degradation behavior and (F) degradation rate of hydrogel in phosphate buffered saline over 14 days. Black arrow shows non-covalent bond. Yellow arrow shows covalent bond. Scale bar = 10  $\mu m$ . Data are presented as mean  $\pm$  standard error of the mean. DMEM/F12: Dulbecco's Modified Eagle Medium and Ham's F-12.

### Fibrin Hydrogel Scaffold Prolongs the Survival of hUC-MSCs in the Peri-Wound Area

Skin wounds were treated with GFP-labeled hUC-MSCs (GFP-hUC-MSCs) or hydrogel-seeded GFP-labeled hUC-MSCs. Immunofluorescence results showed that many

GFP-hUC-MSCs were observed in the lesioned tissue, in both the hUC-MSCs monotherapy (Fig. 3A) and hydrogel-hUC-MSCs combination (Fig. 3B) groups on day 3. However, on day 7, GFP-hUC-MSCs were hardly observed in the lesioned tissue of hUC-MSC monotherapy group (Fig. 3C), while many GFP-hUC-MSCs were still present in

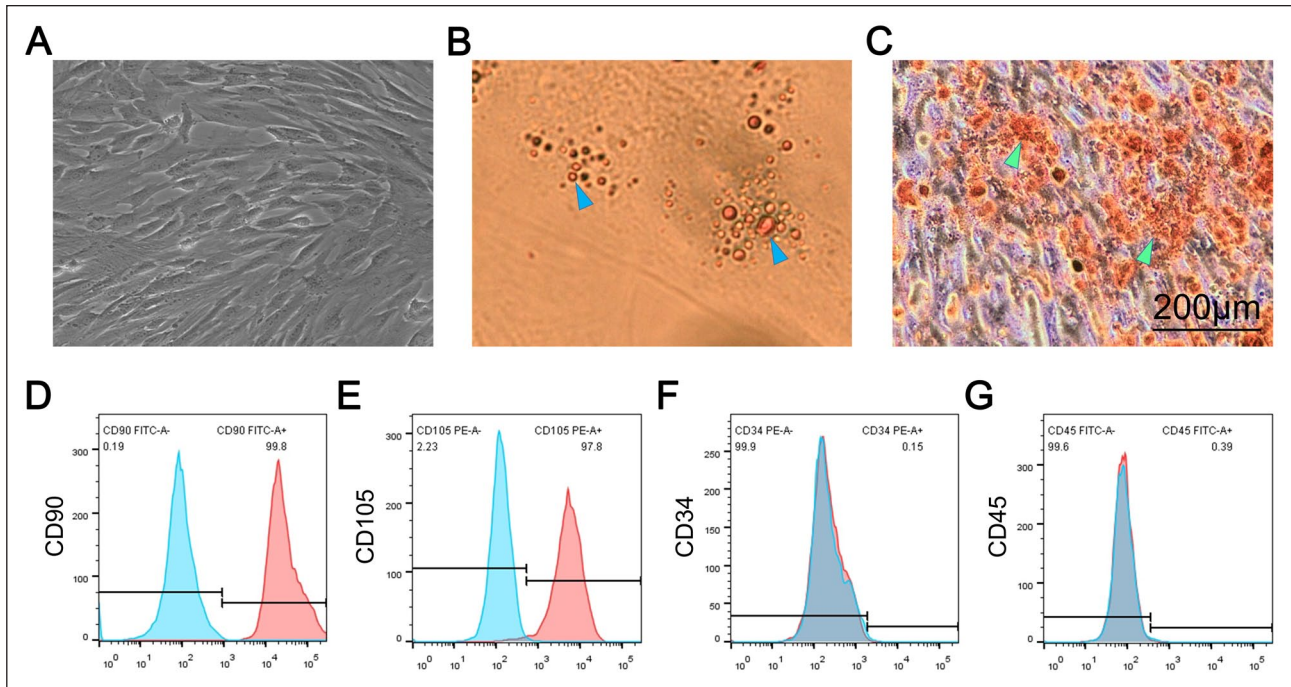


**Figure 2.** hUC-MSCs possess the characteristics of stem cells and multidirectional differentiation potential. (A) Microscopic morphology of hUC-MSCs. (B) Oil red O staining showed formation of lipid droplets (blue arrowheads). (C) Alizarin red staining showed formation of mineralized nodules (green arrowheads). (D–G) Flow cytometric analysis of surface antigens in hUC-MSCs. The blue curves represent isotypic controls. Scale bar = 200  $\mu$ m. hUC-MSCs: Human umbilical cord mesenchymal stem cells.

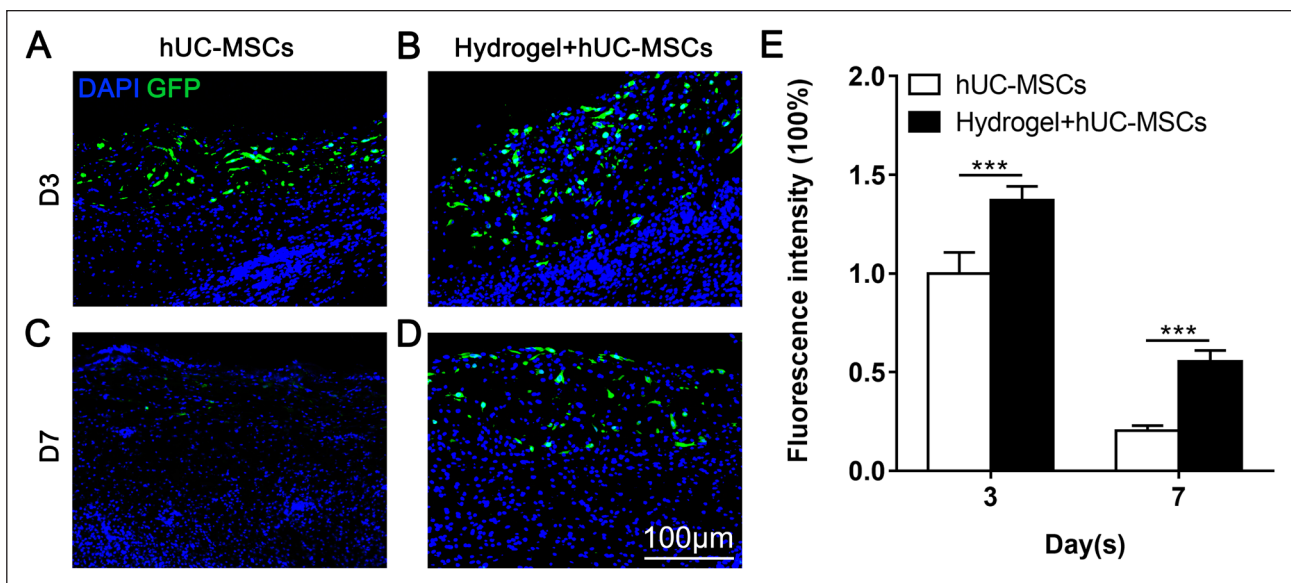


**Figure 3.** Fibrin hydrogel scaffold prolongs the survival time of hUC-MSCs at the wound site. Skin wounds were treated with GFP-labeled hUC-MSCs or hydrogel–GFP-labeled hUC-MSCs. *In vivo* testing—fluorescence tracer results on (A, B) day 3 after surgery (C, D) day 7 after surgery. (E) Comparison of GFP fluorescence intensity between the hUC-MSCs monotherapy and hydrogel–hUC-MSCs combination groups on days 3 and 7 after surgery. Scale bar = 100  $\mu$ m. Data are presented as mean  $\pm$  standard error of the mean. hUC-MSCs: human umbilical cord mesenchymal stem cells; DAPI: 4',6-diamidino-2-phenylindole; GFP: green fluorescent protein. \*\*\* $P$  < 0.001.

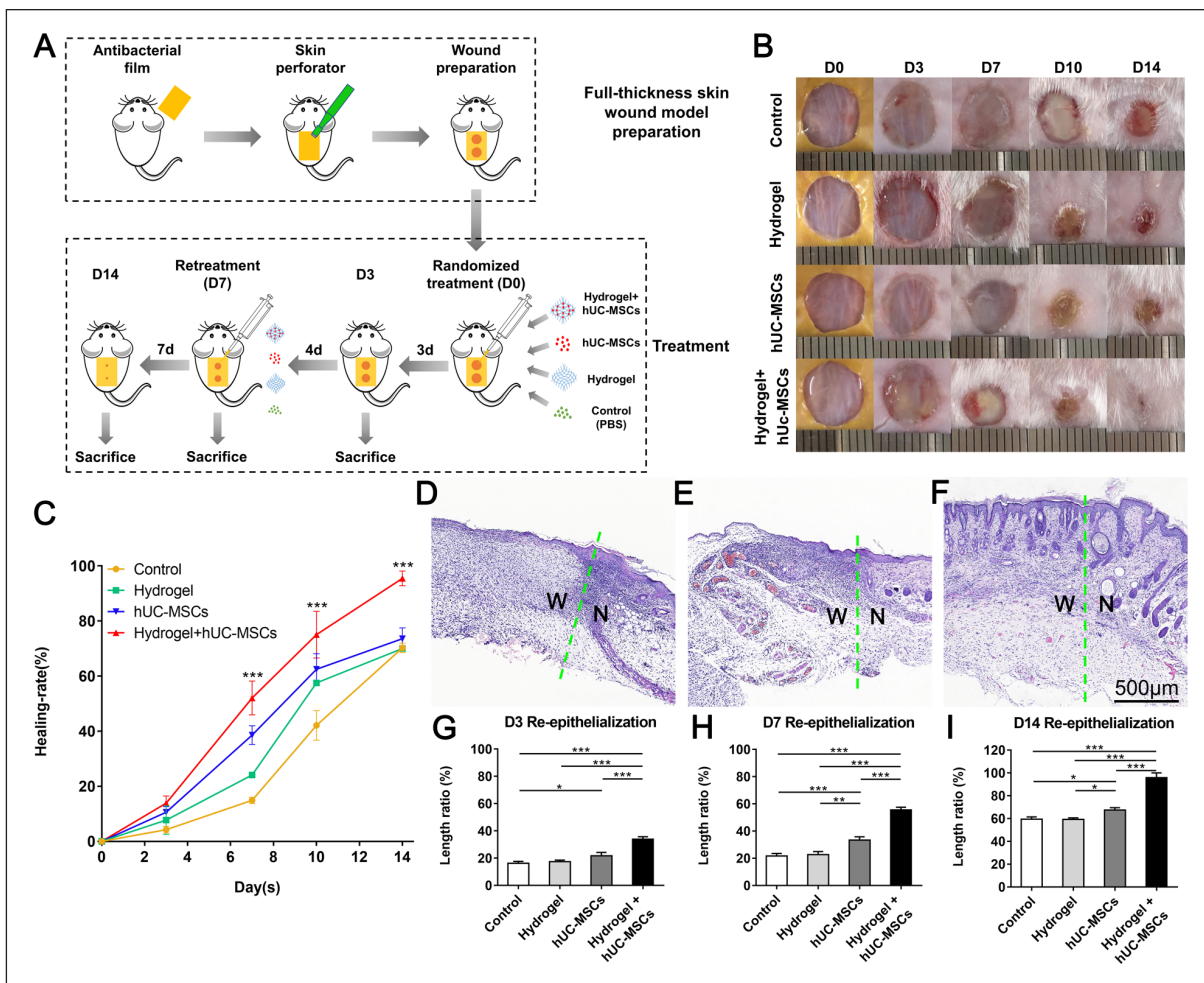


**Figure 4.** Hydrogel–hUC-MSCs combination therapy promotes wound closure. (A) The flow diagram of animal protocol and treatment. (B) Wound healing of mice in the control, hydrogel monotherapy, hUC-MSCs monotherapy, and hydrogel–hUC-MSCs combination groups on days 3, 7, 10, and 14 after surgery. (C) Comparison of wound healing rates among the control, hydrogel monotherapy, hUC-MSCs monotherapy group, and hydrogel–hUC-MSCs combination groups on days 3, 7, 10, and 14 after surgery. (D) H&E staining of the wound in the hydrogel–hUC-MSCs combination group on day 3 after surgery. (E) H&E staining of the wound in the hydrogel–hUC-MSCs combination group on day 7 after surgery. (F) H&E staining of the wound in the hydrogel–hUC-MSCs combination group on day 14 after surgery. (G–I) The ratio of wound re-epithelialization length of the control, hydrogel monotherapy, hUC-MSCs monotherapy and hydrogel–hUC-MSCs combination groups on days 3, 7, and 14 after surgery. Green dotted line shows the edge of the wound. Scale bar = 500  $\mu\text{m}$ . Data are presented as mean  $\pm$  standard error of the mean. H&E: hematoxylin and eosin; hUC-MSCs: human umbilical cord mesenchymal stem cells; W: wound area; N: normal area. \* $P < 0.05$ ; \*\* $P < 0.01$ ; \*\*\* $P < 0.001$ .

the lesioned tissue of hydrogel–hUC-MSC combination group (Fig. 3D). Moreover, GFP fluorescence intensity of the lesioned tissue in the hydrogel–hUC-MSC combination group was higher than that of the lesioned tissue in the hUC-MSCs monotherapy group on days 3 and 7 (Fig. 3E). These results indicated that the fibrin hydrogel scaffold could provide a suitable microenvironment for hUC-MSCs and prolong the survival of hUC-MSCs in the peri-wound area.

#### Hydrogel–hUC-MSCs Combination Therapy Accelerates Wound Closure

All animal experiments and treatments were performed according to standard procedures (Fig. 4A). The efficacy of

the different therapeutic strategies was assessed by observing the postoperative wound healing and calculating the wound healing rates. We found that on days 7, 10, and 14 after the treatment, wounds of mice in the hydrogel–hUC-MSCs combination group healed faster than those of mice in the other three groups. On day 14, the wounds of mice in the hydrogel–hUC-MSCs combination group were almost completely healed, earlier than those of mice in the other three groups (Fig. 4B). Furthermore, the wound healing rate of hydrogel–hUC-MSCs combination group was significantly higher than that of the other three groups from day 7 ( $P < 0.001$ ) (Fig. 4C). On day 3, epidermal cells migrated from the edges of the wounds in the hydrogel–hUC-MSC combination group, forming obvious epithelial tongues (Fig. 4D).

On day 7, epidermal cells in the lesioned tissue of hydrogel–hUC-MSCs combination group continued to proliferate and migrate to the wound (Fig. 4E). On day 14, the skin morphology in samples collected from the hydrogel–hUC-MSCs combination group was almost the same as that of the normal skin tissue (Fig. 4F). Meanwhile, the ratios of wound re-epithelialization length in the hydrogel–hUC-MSCs combination group were all higher than those of the other three groups on days 3, 7, and 14 (Fig. 4G–I). These results suggested that the combination therapy of fibrin hydrogel and hUC-MSCs could accelerate wound closure.

### Hydrogel–hUC-MSCs Combination Therapy Promotes Re-Epithelialization

Immunofluorescence results showed that on days 3 and 7 after surgery, the levels of expression of K10 (Fig. 5A, B) and K14 (Fig. 5C, D), and their extension toward the wound center were higher in the lesioned tissue of hydrogel–hUC-MSCs combination group than those of the other three groups. On day 3, the levels of expression of EGF were higher in the lesioned tissue of hUC-MSC monotherapy and hydrogel–hUC-MSC combination groups than those of the other two groups ( $P < 0.01$  and  $P < 0.05$ , respectively) (Fig. 5E). The level of expression of transforming growth factor  $\beta 1$  (TGF- $\beta 1$ ) was higher in the lesioned tissue of hydrogel–hUC-MSC combination group than that of the other three groups ( $P < 0.01$ ) (Fig. 5H). On days 7 and 14, the levels of expression of EGF and TGF- $\beta 1$  in the lesioned tissue of hydrogel–hUC-MSC combination group were both higher than those in the lesioned tissue of the other three groups ( $P < 0.05$  and  $P < 0.001$ , respectively) (Fig. 5F, G, I, and J, respectively). These results indicated that the combination therapy between fibrin hydrogel and hUC-MSCs could upregulate the expression of EGF and TGF- $\beta 1$  and promote re-epithelialization.

### Hydrogel–hUC-MSCs Combination Therapy Promotes Neovascularization

On day 3 after treatment, we hardly saw any new blood vessels in the samples collected from all four groups (Fig. 6A), and we observed no difference between the levels of expression of VEGFA among them (Fig. 6D). On days 7 and 14, new blood vessels were found in the lesioned tissue of hUC-MSC monotherapy and hydrogel–hUC-MSC combination groups, and they were more abundant than those in the lesioned tissue of the other two groups (Fig. 6B, C, respectively). In addition, the levels of expression of VEGFA were higher in the lesioned tissue of hydrogel–hUC-MSCs combination group than those of the other three groups ( $P < 0.001$ ) (Fig. 6E, F, respectively). These results indicated that the combination therapy between fibrin hydrogel and hUC-MSCs could upregulate the expression of VEGFA and promote neovascularization.

## Discussion

In this study, we describe a fibrin hydrogel scaffold consisting of fibrinogen and thrombin. The scaffold had a porous, three-dimensional mesh structure, and could establish perfectly fitting shapes in irregular wounds.

Full-thickness skin wounds caused by acute trauma, chronic ulcers, and deep burns cause many physiological and functional problems, and are often a therapeutic challenge<sup>4</sup>. Currently, the main therapeutic methods used in clinical practice are functionally limited. For instance, traditional cotton medical gauze has some inevitable disadvantages, such as limited utility, poor absorption properties, and the need of frequent replacement, which may cause secondary trauma. Biological dressings, such as pig skin, carry the risk of spreading bacteria and viruses, and immunological rejection<sup>20–23</sup>. MSCs play important roles in all stages of wound healing<sup>5–9</sup>, but ensuring their survival and effective functioning at the wound site still raises difficulties.

Our previous work demonstrated that the fibrin hydrogel scaffold promotes sustained drug release *in vitro* and *in vivo*<sup>33</sup>. This scaffold not only overcomes the limitations of traditional medical dressings but also provides a suitable microenvironment for hUC-MSCs growth and transplantation for the treatment of skin wounds.

The advantages of hUC-MSCs transplantation in healing skin wounds strongly encourage their use. hUC-MSCs secrete important growth factors necessary for re-epithelialization and angiogenesis through paracrine effect<sup>14–19</sup>. Herein, we found that the fibrin hydrogel scaffold loaded with hUC-MSCs could promote the relative gene expression of growth factors (EGF and VEGFA) and migration-related genes (TGF- $\beta 1$ ), which is beneficial for re-epithelialization, angiogenesis, and extracellular matrix secretion. EGF can stimulate the migration and proliferation of epidermal cells during re-epithelialization<sup>36</sup>. VEGFA, also known as VEGF, is critical for angiogenesis during the formation of the granulation tissue<sup>37</sup>. Newly formed blood vessels can provide regenerating tissues with enough oxygen and nutrition, which are essential to complete wound healing<sup>38</sup>. TGF- $\beta 1$  belongs to the superfamily of TGF $\beta$ , which regulates cell growth and differentiation. It can stimulate fibroblasts to synthesize large amounts of collagen, providing a temporary extracellular matrix for neovascularization, as well as proliferation and migration of basal cells. In addition, TGF- $\beta 1$  can promote fibroblast transformation into myofibroblasts, achieving wound closure<sup>36</sup>. In the present study, the expressions of these cytokines were higher in the lesioned tissue of hydrogel–hUC-MSCs combination therapy group than those of the other treatment groups. Meanwhile, the fluorescence expressions of K10 and K14 were higher in the lesioned tissue of the combination therapy group than those of the other groups. Keratin intermediate filaments are major protein constituents in epithelial cells. They provide mechanical support and fulfill a variety of additional functions<sup>39</sup>. We speculated that the

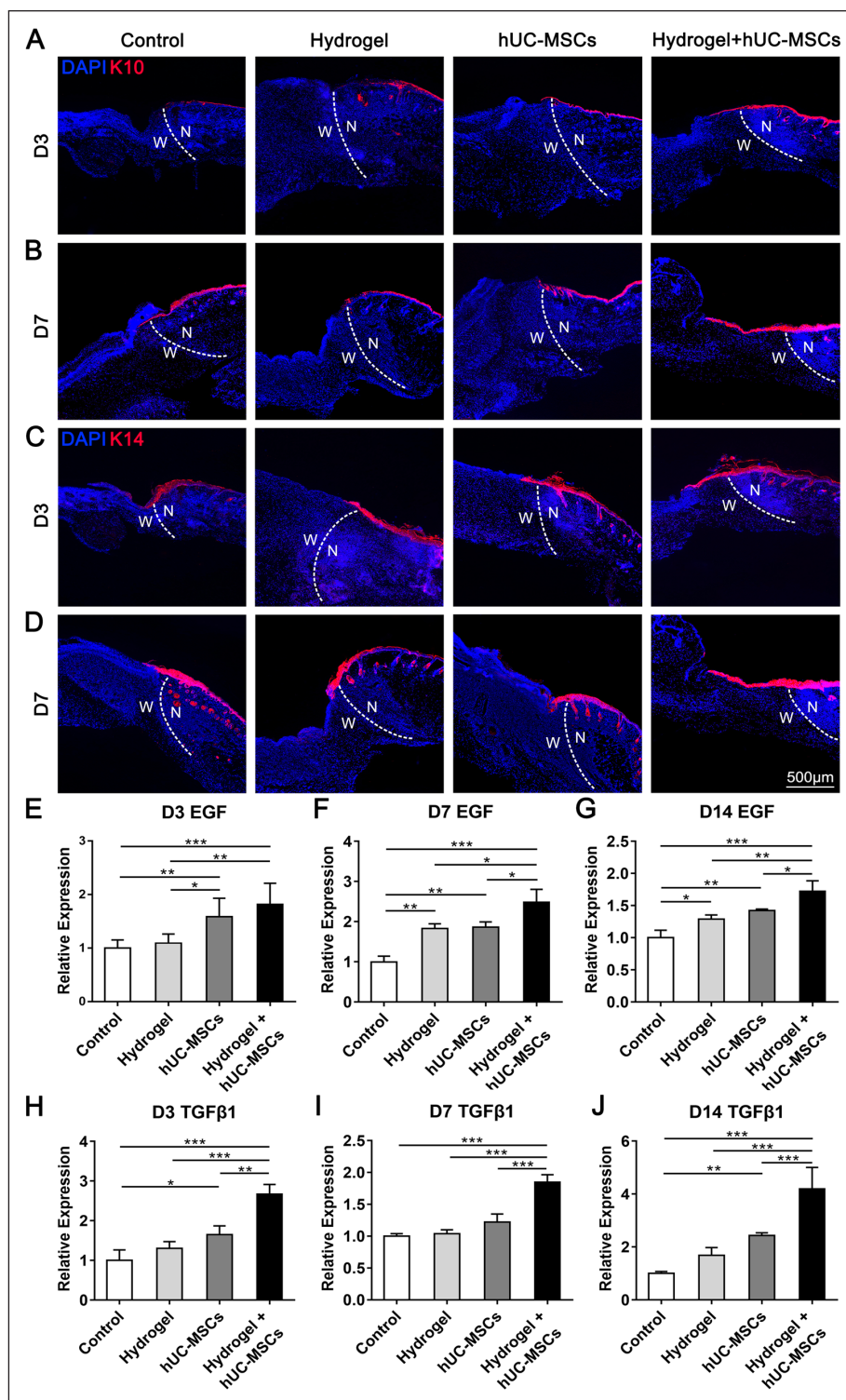


**Figure 5.** Hydrogel-hUC-MSCs combination therapy promotes re-epithelialization. (A, B) Keratin 10 immunofluorescence results of the wounds in the control, hydrogel monotherapy, hUC-MSCs monotherapy, and hydrogel-hUC-MSCs combination groups on days 3 and 7 after surgery. (C, D) Keratin 14 immunofluorescence results of the wounds in the control, hydrogel monotherapy, hUC-MSCs monotherapy, and hydrogel-hUC-MSCs combination groups on days 3 and 7 after surgery. (E-G) Levels of expression of EGF in the in lesioned tissue of control, hydrogel monotherapy, hUC-MSCs monotherapy, and hydrogel-hUC-MSCs combination groups on days 3, 7, and 14 after surgery. (H-J) Levels of expression of TGF-β1 in the in lesioned tissue of control, hydrogel monotherapy, hUC-MSCs monotherapy and hydrogel-hUC-MSCs combination groups on days 3, 7, and 14 after surgery. White dotted line shows the edge of the wound. Scale bar = 500 μm. Data are presented as mean ± standard error of the mean. hUC-MSCs: human umbilical cord mesenchymal stem cells; EGF: epidermal growth factor; TGF-β1: transforming growth factor-β1; W: wound area; N: normal area. \* $P < 0.05$ ; \*\* $P < 0.01$ ; \*\*\* $P < 0.001$ .

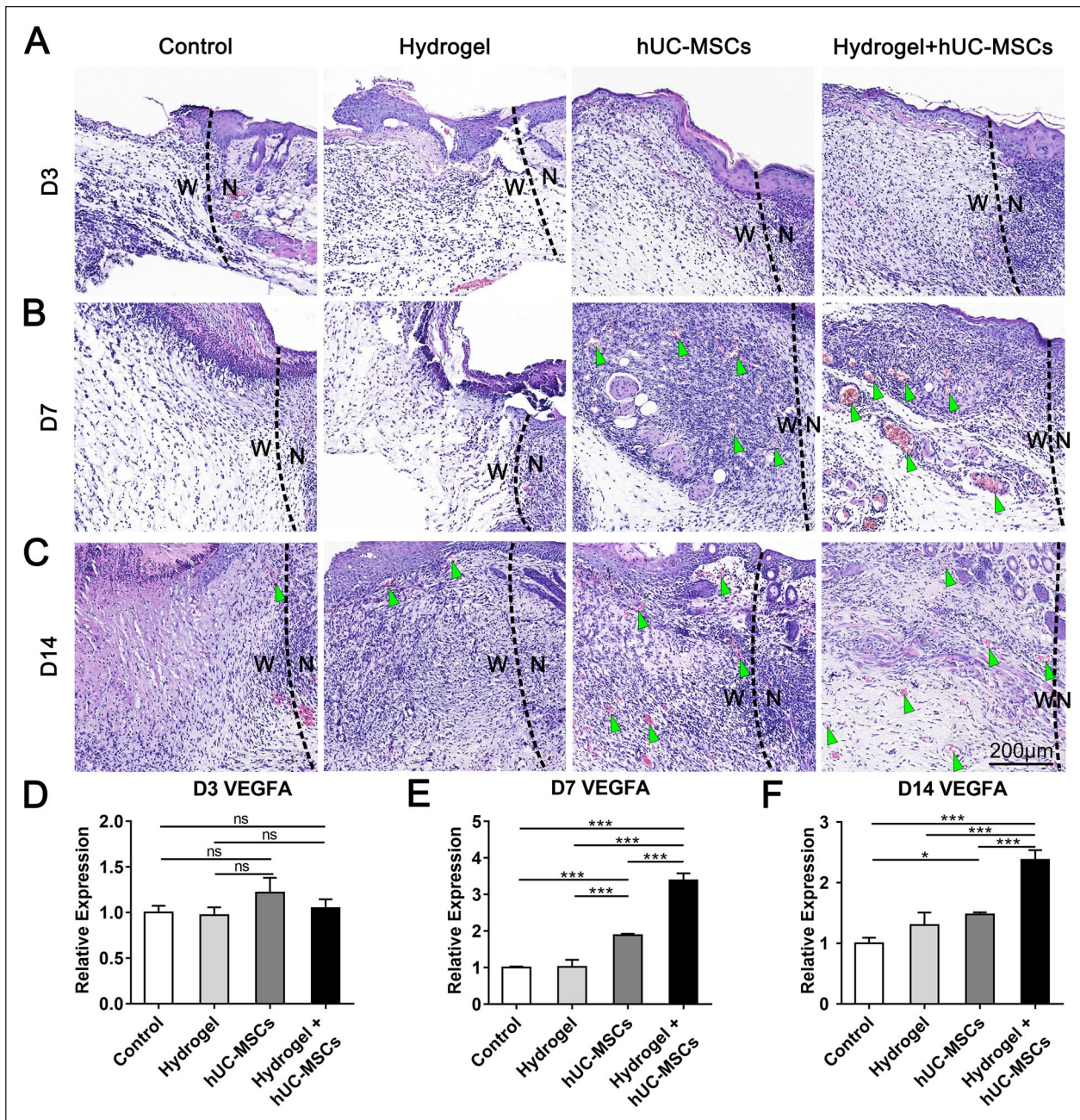


**Figure 6.** Hydrogel–hUC-MSCs combination therapy promotes neovascularization. (A–C) H&E staining of the wounds in the control, hydrogel monotherapy, hUC-MSCs monotherapy, and hydrogel–hUC-MSCs combination groups on days 3, 7, and 14 after surgery. (D–F) Levels of expression of VEGFA in lesioned tissue of the control, hydrogel monotherapy, hUC-MSCs monotherapy, and hydrogel–hUC-MSCs combination groups on days 3, 7, and 14 after surgery. Black dotted line shows the edge of the wound. Green arrowhead shows the blood vessel. Scale bar = 200  $\mu$ m. Data are presented as mean  $\pm$  standard error of the mean. H&E: hematoxylin and eosin; hUC-MSCs: human umbilical cord mesenchymal stem cells; VEGFA: vascular endothelial growth factor A; W: wound area; N: normal area. \* $P < 0.05$ ; \*\* $P < 0.01$ ; \*\*\* $P < 0.001$ .

formation of fibrin hydrogel provided a stable microenvironment for hUC-MSCs allowing them to function better, thus, inducing their paracrine effect and promoting cytokine secretion. With the slow degradation of the hydrogel, cytokines are released enhancing extracellular matrix production,

increasing secretion of cytokines, and improving wound healing. This is a positive feedback regulation.

The ratio of wound re-epithelialization length and the intensity of K10 and K14 immunofluorescence were substantially higher in the lesioned tissue of the

hydrogel–hUC-MSCs combination group than those of the hUC-MSCs monotherapy group. However, on day 3 after surgery, the levels of expression of EGF were similar in the hUC-MSCs monotherapy and hydrogel–hUC-MSCs combination groups. We speculated that hUC-MSCs could not function well without the microenvironment provided by the hydrogel, and thus, the increased expression of EGF in the hUC-MSCs monotherapy group was not enough to recruit sufficient epidermal cells at the wound site. These results further confirm the positive effects of hydrogel on cell adhesion, proliferation, and migration.

These findings strongly support the clinical therapeutic potential of the fibrin hydrogel scaffold loaded with hUC-MSCs. However, this study also has some limitations; thus, the underlying mechanism of how fibrin hydrogel–hUC-MSCs combination therapy promotes wound healing needs further investigation.

## Conclusion

To conclude, we have demonstrated the therapeutic effect of fibrin hydrogel scaffold loaded with hUC-MSCs on full-thickness skin defects. The fibrin hydrogel scaffold can adapt to a variety of irregularly shaped skin wounds. It provides a relatively stable environment for cell adhesion, proliferation, and migration and prolongs cell survival at the wound site. The hydrogel–hUC-MSCs combination therapy has positive effects on the wound closure, re-epithelialization, and neo-vascularization. It exhibits a remarkable therapeutic effect, being more effective than monotherapy with hUC-MSCs or the hydrogel. Our study provides support for using hydrogel–hUC-MSCs combination therapy in the clinical treatment of skin wounds offering a promising strategy for wound healing.

## Author Contributions

Lz Hu, Jh Zhou, and Zs He contributed equally to this work. S Yu, Jz Zhang, and Yg Chen designed the experiments. Lz Hu, Jh Zhou, Zs He, L Zhang, Fz Du, Mt Nie, Y Zhou, H Hao, and Lx Zhang performed the experiments. Lz Hu, S Yu, Jz Zhang, and Yg Chen analyzed the data, wrote the paper, and revised the manuscript. All authors read and approved the final manuscript.

## Ethical Approval

This study protocol was approved by the research Ethics Committee of Suzhou Institute of Biomedical Engineering and Technology, Chinese Academy of Science (IRB No. 2020-D09).

## Statement of Human and Animal Rights

All procedures in this study were conducted in accordance with Suzhou Institute of Biomedical Engineering and Technology, Chinese Academy of Science (IRB No. 2020-D09) approved protocols. All animal procedures were conducted following the provisions of the National Institutes of Health Guide for the Care and Use of Laboratory Animals.

## Statement of Informed Consent

Informed consent was obtained from patients.

## Declaration of Conflicting Interests

The author(s) declared no potential conflicts of interest with respect to the research, authorship, and/or publication of this article.

## Funding

The author(s) disclosed receipt of the following financial support for the research, authorship, and/or publication of this article: This work was supported by National Natural Science Foundation of China (Nos. 81772773, 81400200, 81672560); the Strategic Priority Research Program of the Chinese Academy of Sciences (XDA16020807); the Key Research and Development Program of Jiangsu Province, China (BE2018668, BE2017669); the Social Development Project of Jiangsu Province (BE2021647); Jiangsu Provincial Medical Youth Talent (QNR2016753); the Major Innovative Research Team of Suzhou, China (ZXT2019007); Suzhou Clinical Key Technology Project (LCZX201705); Gusu Medical Youth Talent (GSWS2019034); and The Project of Jiangsu Provincial Maternal and Child Health Association (FYX201709).

## ORCID iD

Lvzhong Hu  <https://orcid.org/0000-0002-2760-8871>

## References

- Zheng Z, Bian S, Li Z, Zhang Z, Liu Y, Zhai X, Pan H, Zhao X. Catechol modified quaternized chitosan enhanced wet adhesive and antibacterial properties of injectable thermo-sensitive hydrogel for wound healing. *Carbohydr Polym.* 2020;249:116826.
- Lei Z, Singh G, Min Z, Shixuan C, Xu K, Pengcheng X, Xueer W, Yinghua C, Lu Z, Lin Z. Bone marrow-derived mesenchymal stem cells laden novel thermo-sensitive hydrogel for the management of severe skin wound healing. *Mater Sci Eng C Mater Biol Appl.* 2018;90:159–67.
- Sadiq A, Shah A, Jeschke MG, Belo C, Qasim Hayat M, Murad S, Amini-Nik S. The role of serotonin during skin healing in post-thermal injury. *Int J Mol Sci.* 2018;19(4):1034.
- Gurtner G, Werner S, Barrandon Y, Longaker M. Wound repair and regeneration. *Nature.* 2008;453(7193):314–21.
- Walter MNM, Wright KT, Fuller HR, MacNeil S, Johnson WEB. Mesenchymal stem cell-conditioned medium accelerates skin wound healing: an in vitro study of fibroblast and keratinocyte scratch assays. *Exp Cell Res.* 2010;316(7):1271–81.
- Jeon YK, Jang YH, Yoo DR, Kim SN, Lee SK, Nam MJ. Mesenchymal stem cells' interaction with skin: wound-healing effect on fibroblast cells and skin tissue. *Wound Repair Regen.* 2010;18(6):655–61.
- Luo G, Cheng W, He W, Wang X, Tan J, Fitzgerald M, Li X, Wu J. Promotion of cutaneous wound healing by local application of mesenchymal stem cells derived from human umbilical cord blood. *Wound Repair Regen.* 2010;18(5):506–13.
- Schlosser S, Dennler C, Schweizer R, Eberli D, Stein JV, Enzmann V, Giovanoli P, Erni D, Plock JA. Paracrine effects of mesenchymal stem cells enhance vascular regeneration in ischemic murine skin. *Microvasc Res.* 2012;83(3):267–75.

9. Gu J, Liu N, Yang X, Feng Z, Qi F. Adipose-derived stem cells seeded on PLCL/P123 electrospun nanofibrous scaffold enhance wound healing. *Biomed Mater*. 2014;9(3):035012.
10. Lee DE, Ayoub N, Agrawal DK. Mesenchymal stem cells and cutaneous wound healing: novel methods to increase cell delivery and therapeutic efficacy. *Stem Cell Res Ther*. 2016;7:37.
11. Ding DC, Chang YH, Shyu WC, Lin SZ. Human umbilical cord mesenchymal stem cells: a new era for stem cell therapy. *Cell Transplant*. 2015;24(3):339–47.
12. Shi Y, Wang Y, Li Q, Liu K, Hou J, Shao C, Wang Y. Immunoregulatory mechanisms of mesenchymal stem and stromal cells in inflammatory diseases. *Nat Rev Nephrol*. 2018;14(8):493–507.
13. Li S, Wang Y, Guan L, Ji M. Characteristics of human umbilical cord mesenchymal stem cells during ex vivo expansion. *Mol Med Rep*. 2015;12(3):4320–25.
14. Detamore MS. Human umbilical cord mesenchymal stromal cells in regenerative medicine. *Stem Cell Res Ther*. 2013;4(6):142.
15. Qin HL, Zhu XH, Zhang B, Zhou L, Wang WY. Clinical evaluation of human umbilical cord mesenchymal stem cell transplantation after angioplasty for diabetic foot. *Exp Clin Endocrinol Diabetes*. 2016;124:497–503.
16. Yang J, Chen Z, Pan D, Li H, Shen J. Umbilical cord-derived mesenchymal stem cell-derived exosomes combined pluronic F127 hydrogel promote chronic diabetic wound healing and complete skin regeneration. *Int J Nanomedicine*. 2020;15:5911–26.
17. Liu L, Yu Y, Hou Y, Chai J, Duan H, Chu W, Zhang H, Hu Q, Du J. Human umbilical cord mesenchymal stem cells transplantation promotes cutaneous wound healing of severe burned rats. *PLoS ONE*. 2014;9(2):e88348.
18. Shi H, Xu X, Zhang B, Xu J, Pan Z, Gong A, Zhang X, Li R, Sun Y, Yan Y, Mao F, et al. 3,3'-Diindolylmethane stimulates exosomal Wnt11 autocrine signaling in human umbilical cord mesenchymal stem cells to enhance wound healing. *Theranostics*. 2017;7(6):1674–88.
19. Wang S, Yang H, Tang Z, Long G, Huang W. Wound dressing model of human umbilical cord mesenchymal stem cells-alginate complex promotes skin wound healing by paracrine signaling. *Stem Cells Int*. 2016;2016:3269267.
20. Priya SG, Jungvid H, Kumar A. Skin tissue engineering for tissue repair and regeneration. *Tissue Eng Part B Rev*. 2008;14(1):105–18.
21. Dini V, Romanelli M, Piaggese A, Stefani A, Mosca F. Cutaneous tissue engineering and lower extremity wounds (part 2). *Int J Low Extrem Wounds*. 2006;5(1):27–34.
22. Garlick JA. Engineering skin to study human disease—tissue models for cancer biology and wound repair. *Adv Biochem Eng Biotechnol*. 2007;103:207–39.
23. Macri L, Clark RAF. Tissue engineering for cutaneous wounds: selecting the proper time and space for growth factors, cells and the extracellular matrix. *Skin Pharmacol Physiol*. 2009;22(2):83–93.
24. Sun Y, Nan D, Jin H, Qu X. Recent advances of injectable hydrogels for drug delivery and tissue engineering applications. *Polym Test*. 2020;81:106283.
25. Drury JL, Mooney DJ. Hydrogels for tissue engineering: scaffold design variables and applications. *Biomaterials*. 2003;24(24):4337–51.
26. Mehrali M, Thakur A, Pennisi CP, Talebian S, Arpanaei A, Nikkhah M, Dolatshahi-Pirouz A. Nanoreinforced hydrogels for tissue engineering: biomaterials that are compatible with load-bearing and electroactive tissues. *Adv Mater*. 2017;29(8):1603612.
27. Sivashanmugam A, Arun Kumar R, Vishnu Priya M, Nair SV, Jayakumar R. An overview of injectable polymeric hydrogels for tissue engineering. *Eur Polym J*. 2015;72:543–65.
28. Alexander A, Ajazuddin Khan J, Saraf S, Saraf S. Poly(ethylene glycol)-poly(lactic-co-glycolic acid) based thermosensitive injectable hydrogels for biomedical applications. *J Control Release*. 2013;172(3):715–29.
29. Kopecek J. Hydrogel biomaterials: a smart future? *Biomaterials*. 2007;28(34):5185–92.
30. Tsou YH, Khoneisser J, Huang PC, Xu X. Hydrogel as a bioactive material to regulate stem cell fate. *Bioact Mater*. 2016;1(1):39–55.
31. Chen Q, Wang C, Zhang X, Chen G, Hu Q, Li H, Wang J, Wen D, Zhang Y, Lu Y, Yang G, et al. In situ sprayed bioresponsive immunotherapeutic gel for post-surgical cancer treatment. *Nat Nanotechnol*. 2019;14(1):89–97.
32. Losi P, Briganti E, Errico C, Lisella A, Sanguinetti E, Chiellini F, Soldani G. Fibrin-based scaffold incorporating VEGF- and bFGF-loaded nanoparticles stimulates wound healing in diabetic mice. *Acta Biomater*. 2013;9(8):7814–21.
33. Zhang L, Zhou J, Hu L, Han X, Zou X, Chen Q, Chen Y, Liu Z, Wang C. In situ formed fibrin scaffold with cyclophosphamide to synergize with immune checkpoint blockade for inhibition of cancer recurrence after surgery. *Adv Funct Mater*. 2019;30(7):1906922.
34. Zhang L, Yan X, An L, Wang M, Xu X, Ma Z, Nie M, Du F, Zhang J, Yu S. Novel pneumatically assisted atomization device for living cell delivery: application of sprayed mesenchymal stem cells for skin regeneration. *Bio-Des Manuf*. 2022;5(1):220–32.
35. Xu L, Ding L, Wang L, Cao Y, Zhu H, Lu J, Li X, Song T, Hu Y, Dai J. Umbilical cord-derived mesenchymal stem cells on scaffolds facilitate collagen degradation via upregulation of MMP-9 in rat uterine scars. *Stem Cell Res Ther*. 2017;8(1):84.
36. Singer A, Clark R. Cutaneous wound healing. *New Eng J Med*. 1999;341(10):738–46.
37. Nissen NN, Polverini PJ, Koch AE, Volin MV, Gamelli RL, DiPietro LA. Vascular endothelial growth factor mediates angiogenic activity during the proliferative phase of wound healing. *Am J Pathol*. 1998;152(6):1445–52.
38. Chen S, Wang H, Su Y, John JV, McCarthy A, Wong SL, Xie J. Mesenchymal stem cell-laden, personalized 3D scaffolds with controlled structure and fiber alignment promote diabetic wound healing. *Acta Biomater*. 2020;108:153–67.
39. Schweizer J, Bowden PE, Coulombe PA, Langbein L, Lane EB, Magin TM, Maltais L, Omary MB, Parry DA, Rogers MA, Wright MW. New consensus nomenclature for mammalian keratins. *J Cell Biol*. 2006;174(2):169–74.